AGU PUBLICATIONS

JGR

Journal of Geophysical Research: Oceans

RESEARCH ARTICLE

10.1002/2016JC012524

Sea ice growth rates from tide-driven visible banding

Kate E. Turner[1], Inga J. Smith[2], Jean-Louis Tison[3], Véronique Verbeke[3,4], Mark McGuinness[5], Malcolm Ingham[1], Ross Vennell[6], and Joe Trodahl[1,7]

[1]School of Chemical and Physical Sciences, Victoria University of Wellington, Wellington, New Zealand, [2]Department of Physics, University of Otago, Dunedin, New Zealand, [3]Laboratoire de Glaciologie (DGES), Université Libre de Bruxelles, Brussels, Belgium, [4]Quality of the Environment and Nature Management Division, Brussels Environment, Brussels, Belgium, [5]School of Mathematics and Statistics, Victoria University of Wellington, Wellington, New Zealand, [6]Department of Marine Science, University of Otago, Dunedin, New Zealand, [7]MacDiarmid Institute for Advanced Materials and Nanotechnology, Victoria University of Wellington, Wellington, New Zealand

Abstract In this paper, periodic tide-current-driven banding in a sea-ice core is demonstrated as a measure of the growth rate of first-year sea ice at congelation-ice depths. The study was performed on a core from the eastern McMurdo Sound, exploiting the well-characterized tidal pattern at the site. It points the way to a technique for determining early-season ice growth rates from late-season cores, in areas where under ice currents are known to be tidally dominated and the ice is landfast, thus providing data for a time of year when thin ice prevents direct thickness (and therefore growth rate) measurements. The measured results were compared to the growth-versus-depth predicted by a thermodynamic model.

Plain Language Summary It is currently very difficult to measure sea-ice growth rates, due to the danger of traveling on thin ice early in the growing season. This paper introduces the use of tidal patterns to determine sea-ice growth rates at the end of the growing season, when ice cores can be taken. The technique utilizes the visible light and dark bands that are often present in sea ice near land, and are driven by changes in the tidal current beneath the ice. As well as being important for climate research, this method could contribute to the understanding biological ecosystems within the ice, by providing a method to date depths in an ice core where particular organisms are observed or samples taken.

Key Points:
- Visible banding in congelation ice linked to periodic tidal currents
- Early season sea-ice growth rates versus depth estimated directly from banding present in first-year sea-ice cores from McMurdo Sound Antarctica
- Growth rates related to total freezing time using simple ice growth model

Supporting Information:
- Supporting Information S1
- Data Set S1
- Figure S1

Correspondence to:
K. Turner,
turner.kate@outlook.com

Citation:
Turner, K. E., I. J. Smith, J.-L. Tison, V. Verbeke, M. McGuinness, M. Ingham, R. Vennell, and J. Trodahl (2017), Sea ice growth rates from tide-driven visible banding, *J. Geophys. Res. Oceans*, *122*, 4675–4684, doi:10.1002/2016JC012524.

Received 5 NOV 2016
Accepted 12 APR 2017
Accepted article online 21 APR 2017
Published online 8 JUN 2017

1. Introduction

The growth processes of first-year sea ice are of importance for determining the energy balance of ice-covered oceans. There exist sea-ice growth rate data late in the growth season at a few locations in Antarctica, but earlier data are sparse due to danger of travel until ice is sufficiently thick. In addition, remote sensing of sea-ice thickness (and therefore growth rates) is difficult for thin ice [*Mäkynen and Similä*, 2015]. Growth rates of thin sea ice are particularly important in a warming climate where they may be affected by temperature and precipitation changes. There is then a premium to be placed on techniques that permit growth measurements in the early part of the growth season when there is relatively rapid heat exchange with the atmosphere and high growth rates for thin ice. Here we describe the use of periodic tide-current-driven visible bands in first-year sea ice as a marker to determine growth rates in the first two months after the formation of a continuous ice cover.

Visible horizontal banding is apparent in cores collected from the sea-ice cover in many near-coastal first-year sea-ice sites [*Cole et al*., 2004]. Ultimately, visible bands are variations in the degree of optical scattering throughout the depths of the ice, caused by fluctuations in the size and density of brine inclusions, and concentrations of soluble gases, and salts [*Cole et al*., 2004; *Eicken et al*., 2000; *Light et al*., 2003]. Both experimental [*Eicken et al*., 2000; *Verbeke et al*., 2002] and theoretical [*McGuinness*, 2009] considerations indicate that these properties are influenced by under ice currents, which drive turbulent mixing in concentrated brine rejected at the growing face. Within that mechanism, the banding thus signals varying current speeds during the ice growth. Oceanic currents are in turn influenced by many things, but the very clearly periodic

banding commonly seen near land masses immediately suggests that they are driven by tidal-current speed variations. Exactly such periodic banding is illustrated in the core in Figure 1 on which the present research is based. The relationship to periodic tidal currents provides the time stamp with which growth rates have been determined.

The core in Figure 1 was extracted in November 1999 from McMurdo Sound, where currents are dominated by the tidal cycle [*Leonard et al*., 2006]. The tidal pattern in the eastern McMurdo Sound is especially simple, since the tides off the southern tip of Hut Point are almost fully diurnal (i.e., with one high and one low tide per day) [*Doodson*, 1924; *Heath*, 1971a]. The banding is related to the tide current speed, rather than height, for which there are no direct data available, but which one normally expects to peak during both the ebb and flow with a periodicity of about 12–12.5 h. The proximity of the site to McMurdo Station and Scott Base ensures that there exist considerable data concerning tidal patterns [*Heath*, 1971a,1971b; *Doodson*, 1924]; the tide heights predicted by a model during the period early in 1999 are seen in Figure 2. The reduced range of tidal currents during neap tides is expected to be associated with a weakening or absence of banding. Spring tides, in contrast, have periods of relatively fast currents and periods of quiescent flow, resulting in distinct contrasts between parts of the tidal cycle.

In the present work, we report an analysis of the banding in Figure 1 to provide an early-growth-season growth rate. Our assignment of periodic tidal currents as the driving force behind periodic banding is central to the analysis, and nonperiodic banding mechanisms are not considered in this paper. We note that light variations are weak, since the sun is below the horizon for essentially the entire time to which the analysis is applied, and that leads in turn to negligible daily, as opposed to weather-driven, temperature variations [*Verbeke et al*., 2002]. These are further limited by light absorption in especially the infrared regime [*Haines et al*., 1997] and by thermal diffusivity attenuation of temperature fluctuations [*Trodahl et al*., 2000]. In view of the ∼25 h period of the tides in McMurdo Sound, the most likely periodic tide *current* period is ∼12.5 h, though double that would be appropriate if there is a strong contrast between ebb and flow. Below we perform the analysis assuming 12.5 h, and subsequently demonstrate that a 25 h period is inconsistent with the freeze-in date and a direct thickness measurement performed after the ice was safe for travel. The 12.5 h period is then assessed by comparing the resultant growth rates with several events that are expected to significantly influence the ice growth: neap tides and a period of considerable atmospheric warming.

1.1. Background Information on Core and Tidal Data

The ice core analyzed here was extracted ∼1 km offshore near Arrival Heights in Antarctica in 1999 at a site 150 m away from a thermistor string at a latitude/longitude of 77°50.197′S, 166°36.764′E. The 1999 site [*Smith et al*., 2001] and thermistor string results for ice that year that grew later than that considered here [*Trodahl et al*., 2001] have been described previously. *Verbeke et al*. [2002] established that the white layers in Figure 1 were correlated with enhanced chlorinity and gas (CO_2, O_2, N_2) concentrations, and increased salinity; those data were published in that paper. Although that earlier report identified tidal currents as driving the banding pattern, no attempt was made to invert the problem, i.e., to determine growth rates from the periodic banding. That extension is the subject of the present study. Further, *Verbeke et al*. [2002] postulated a 25 h banding period; in this paper, we show that that was incorrect.

The treatment of the core after extraction and the details of the photography were described fully in an earlier discussion of the banding characteristics [*Verbeke et al*., 2002]. In Figure 1 we reproduce the core photographs, three images of the top 1200 mm followed by three images covering ∼1200 to ∼2200 mm depth. The various core sections of typically 150–300 mm length were assembled at their natural breaks and sequentially sawn in half. From the left the images are of the following: the two halves under front lighting (first image from the left); transmission through one of the half cores after being further sawn into a thick section (second image); a cross-polarized image of this section after further thinning to reveal the crystalline structure of the congelation ice (third image). The lower images on the right compare banding at two sites separated by ∼10 m.

The tidal pattern shown in Figure 2, used to interpret the banding, is from a model using tidal constituents based on tide gauge data taken off Hut Point/Arrival Heights. The tidal cycle has a period of ∼25 h with a strong contrast between ∼1 m and < 0.1 m amplitudes in spring and neap tides, respectively. Measured near-surface horizontal current speeds for a similar site and month in McMurdo Sound give reasonable bounds for reference:

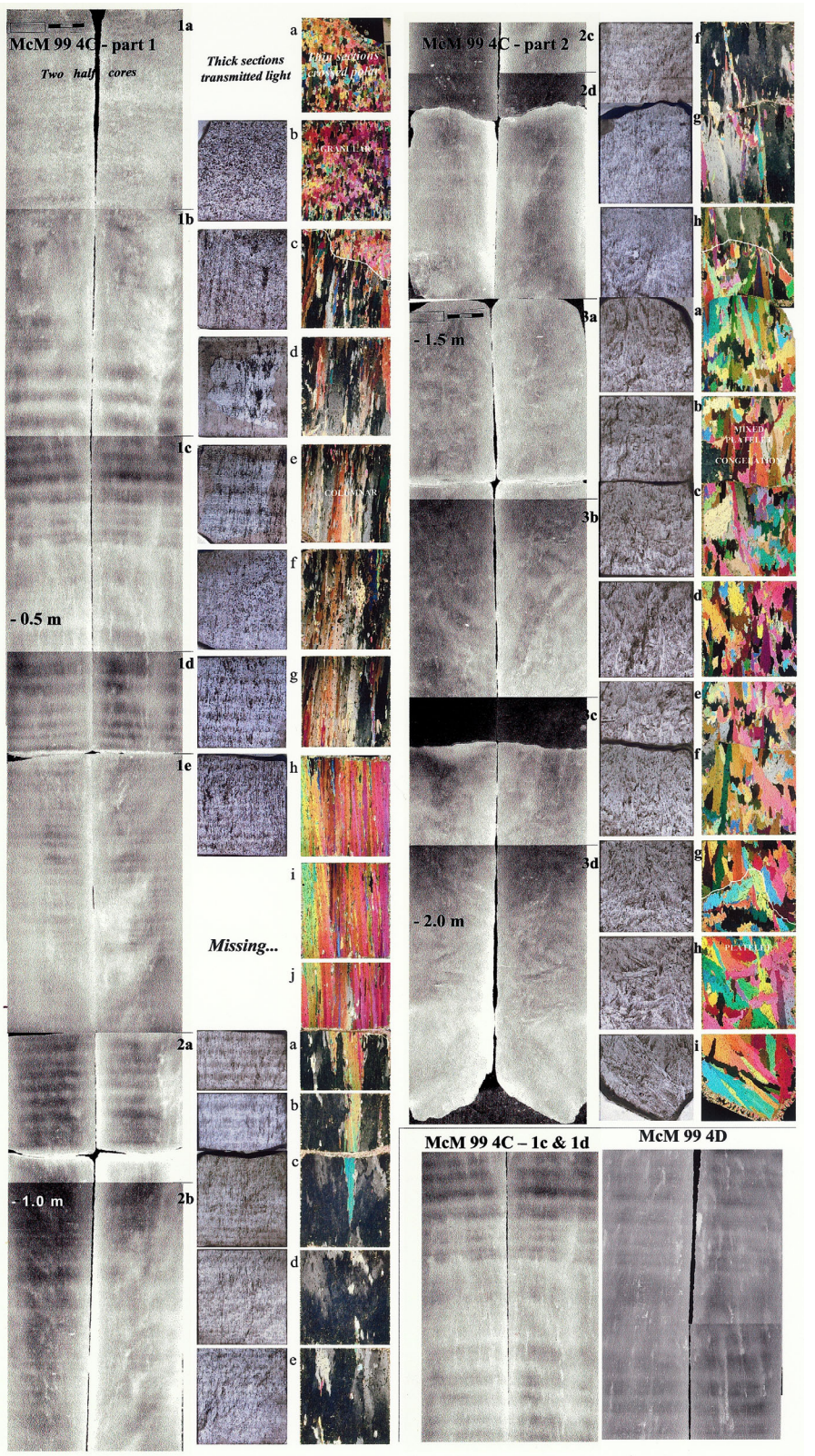

Figure 1. Core photographs used in this work, covering 0–1200 mm depth in the three leftmost images, and deeper parts of the core in the rightmost three images. The leftmost image in each set of three are of the two half cylinders, the second is under transmitted light through a thick (5 mm) slab and the third is of thin (0.6 mm) sections of ice in transmission through crossed polarizers, showing evidence of congelation ice between 150 and 1400 mm. The half-cylinder images in the lower right show close agreement between the banding patterns on two cores taken a few meters apart. Reproduced in color from image published in black and white as Figure 1 in *Verbeke et al.* [2002].

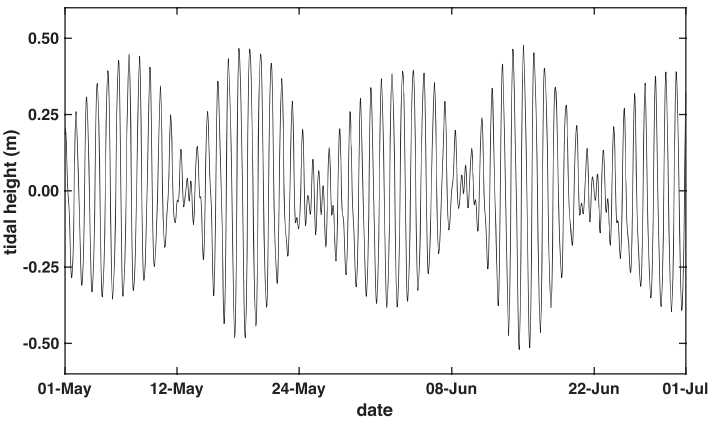

Figure 2. Tidal height for McMurdo Sound for May and June 1999. Note especially the dominant 25 h period and the dates of neap tides: 13 and 25 May, 8 and 22 June.

a maximum current speed of 0.2 m s^{-1} during spring tides and 0.1 m s^{-1} during neap tides [*Leonard et al*., 2006]. We can then reasonably assume that the current speed, peaking once during both the ebb and the flow, will have a period of ~12.5 h, though local bathymetry will determine when in the tidal cycle these peaks occur.

2. Banding Analysis

In the cross-polarized images, it is clear that the granular ice solidified when it was about 150 mm thick, and thereafter the pattern is that of congelation ice. Below a depth of 1400 mm, the crystalline pattern of congelation ice changed, signaling the incorporation of platelet ice [*Smith et al*., 1999, 2001], which is associated with a negative oceanic heat flux [*Trodahl et al*., 2000]. It is fortunate in the context of the present study that supercooled melt water from the Ross Ice Shelf does not appear in the eastern McMurdo Sound until late July or August, for the associated platelet ice that forms, disturbs the growth kinetics and eliminates visible banding [*Leonard et al*., 2006; *Mahoney et al*., 2011]. Thus it is only below 150 mm and above 1400 mm that the tidal speed patterns are revealed by banding. Within that range banding is clearly visible at many depths, though with an opportunity for confusion associated with the joins between adjacent sections of the core; the impact of these joins on the results is discussed below. Nonetheless there are depths at which banding is clearly seen in both the half cylinders and the thick sections, and it is these that we have exploited.

A corresponding image of the leftmost half-cylinder photograph of Figure 1 (supporting information Figure S1) was digitized by reading the image into MATLAB 8.5 using the function imread, averaging the RGB intensity in pixels to improve the signal-to-noise ratio, and smoothed using a median filter in the depth direction. The depth filter was applied over a range of 15 pixels, which corresponds to a depth of 2.8 mm. The thicknesses of the bands range from 24 to 4 mm, with the effect at depth, where the bands are the closest together, being a decrease in the amplitude of the signal. These data were then summed across the ice layer; Figure 3 illustrates the trace of the depth-dependent relative opacity. There are clear, nearly periodic banding patterns, though the image analysis is severely disturbed by the breaks between core sections (approximately every 150–300 mm), which then mask the banding near those breaks. The digitized banding trace was expanded across a short depth span as shown in Figure 3, which also illustrates the determination of growth rate. We measured the depth separation, Δz, corresponding to equivalent midpoints of the oscillations seen in the trace, and calculated the rate at the midpoint as $\Delta z/12.5$ h. Note that this in principle gives growth rate averaged over 12.5 h, and provides one such average every 6.25 h. We show the results from the reliably resolved banding, for which we estimate the uncertainty as typically ± 3 mm/d. The growth rate is shown plotted against depth in Figure 4.

The transformation of the depth to a time scale requires independently determined fixed points. An ice thickness of 1100 mm was directly measured on 21 June at the nearby thermistor string site [*Smith et al*., 2012], when it was deemed safe enough to access the site. In principle, thickness for all dates can then be determined by integrating the growth rate data back from that point, though the growth-rate uncertainties and gaps in the banding data prevent that as a practical procedure. The date of fully stable freeze-over would provide another firm reference depth/date point, but satellite images that might allow that option show only that the ice did not form until sometime after 1 May [*Falconer and Pyne*, 2004]. However, a first-order approximation can be based on recognizing that for a constant temperature difference across the ice, the growth rate varies inversely with the thickness as:

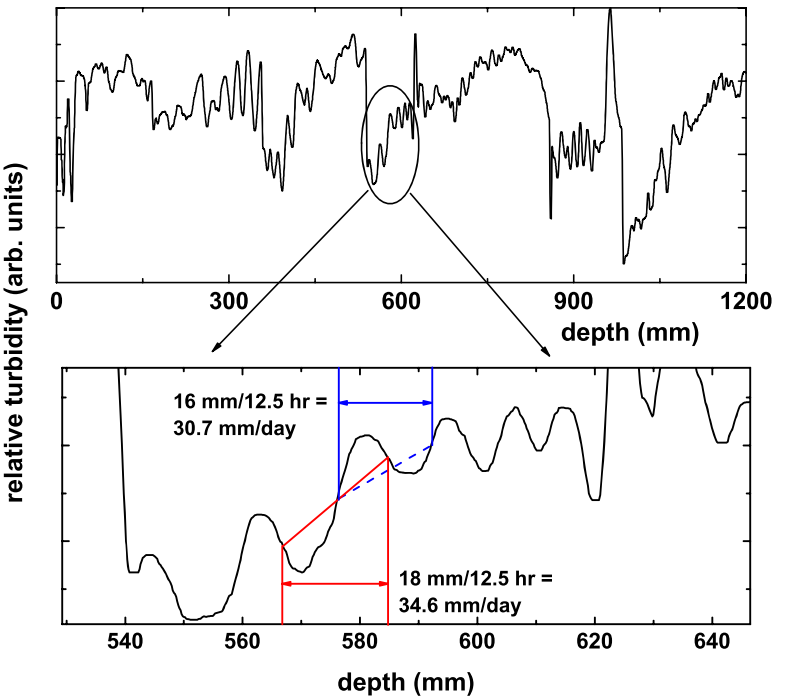

Figure 3. The opacity signaled by the banding pattern versus depth. The sharp offsets are all related to depths at which the core broke in extraction, leading to sudden changes in backscattered and transmitted light. Strong periodic banding is seen at many depths, with periods estimated by measuring the separation of equivalent phases in the opacity variation, as illustrated in the expanded graph across the 600 mm depth. See text for details on the blue and red curve treatments.

$$\frac{dH}{dt} = \frac{k_{si}}{\rho_{si} L} \frac{(T_w - T_s)}{H} \tag{1}$$

where k_{si} is the thermal conductivity of the ice, L is the latent heat of fusion, and ρ_{si} is the ice density. Thus the product of the growth rate dH/dt and the thickness H is expected to scale approximately as the difference between the temperature of the seawater T_w (−1.9°C) and that of the ice surface T_s. The resulting graph is shown in Figure 5, yielding surface temperatures in the reasonable range of −15 to −36°C. It is important to note that the surface temperature returned by this process is an average over a time interval given by the thermal diffusivity through the ice cover, ∼1 day. The product HdH/dt in Figure 5 is centered on $\sim 1.35 \times 10^4$ mm^2/d. Using that value, the inferred time for the ice to grow from the 150 mm granular ice interface to a thickness of 1100 mm is then 44 days, and the resulting freeze in date is ∼8 May.

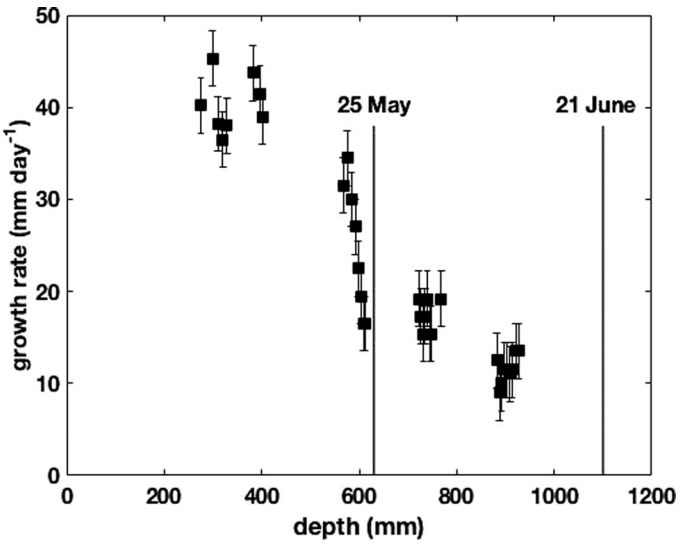

Figure 4. Banding-determined growth rates versus depth (supporting information data set S1). The vertical lines represent the assignment we have made for the neap tide on 25 May below, and the directly measured depth on 21 June. Congelation ice formation started at 150 mm.

It is now possible to demonstrate the inconsistency that results for an assumed 25 h tidal flow period suggested in the earlier paper of *Verbeke et al.* [2002]. Assuming that banding period, the growth rate estimate is a factor of 2 smaller.

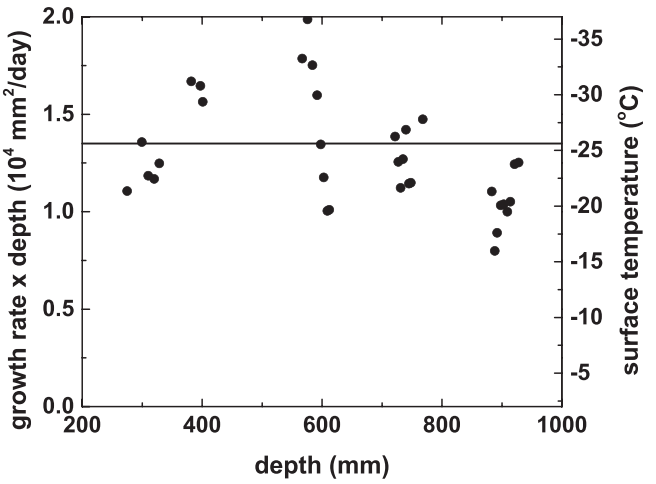

Figure 5. The product of the growth rate and depth data. Our simple model says this product should match the implied surface temperature indicated by the right-hand vertical axis. An approximate center point of this product, indicated by the solid line, provides the means to eliminate from consideration the 25 h banding period, as postulated by *Verbeke et al*. [2002].

This implies that the ice surface temperature is in the range of −9 to −19°C, which is unreasonably warm, and the freeze-in date is 88 days before 21 June (i.e., 25 March). Satellite images, however, show open water long after that date [*Falconer and Pyne*, 2004], in clear disagreement with the slower growth rate. The 25 h banding period evidently resulted from an interpretation of only the most clearly visible banding, biasing the results toward the shallower depths showing the most rapid growth. In analyzing the banding, the semiautomated digitizing technique presented in this paper is therefore superior to the method employed in the *Verbeke et al*. [2002] analysis.

A further fixed point is available by noting that the sudden growth reduction near 600 mm thickness correlates with a strong air temperature rise on 20–22 May as seen in the air temperature record (Figure 6) for the nearby Scott Base electronic weather station [*National Institute of Water and Atmospheric Research*, n.d.]. Air temperature close to the ice surface is sufficiently similar to the ice surface temperature averaged over large spatial scales [*Yu and Rothrock*, 1996] for air temperature variations to be treated as a proxy for surface temperature variations in this case. The rise in the air temperature is therefore used to date the obvious decrease in growth rate seen in the trace. The thermal diffusivity of sea ice introduces a delay before the surface temperature affects the growth rate (see Appendix A) so that one expects the growth rate at 600 mm depth to fall a day or two later than a surface temperature rise. Neap tides occurred in mid-1999 around 13 and 25 May, 8 and 22 June, as seen in Figure 2. Thus for the warmer temperature to affect the ice at a depth of 600 mm, the neap tide on 25 May occurred in the banding-free depth just below the rapid growth reduction, as shown in Figure 3. The growth rate in the 600–800 mm depths then indicates that the neap tide on 8 June corresponds to a depth of ∼870 mm, and the growth rates at shallower depths, coupled with depth of the 25 May neap tide, suggests a freeze-over date of about 11 May.

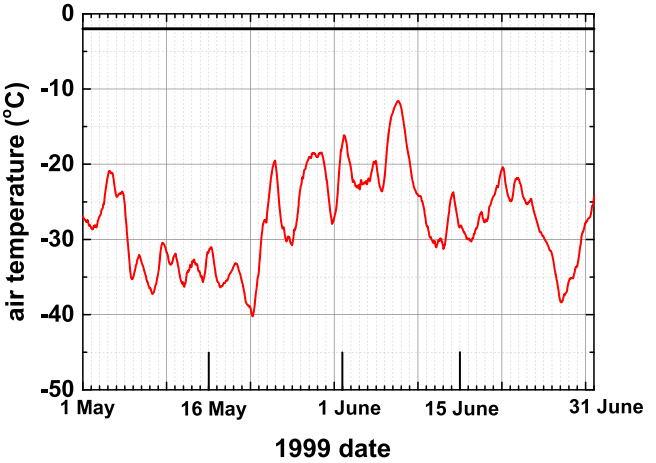

Figure 6. Air temperature versus time at Scott Base through mid-1999 [*National Institute of Water and Atmospheric Research*, n.d.]. The horizontal line at the top indicates a sea temperature of −1.9°C at the base of the ice, assuming constant salinity. Note especially the sudden temperature rise occurring between 20 and 22 May, which correlates with a rapid sea-ice growth reduction near 600 mm thickness.

This estimate of 11 May is the result of the method developed through each of the previous steps in the analysis; satellite images showed that freeze over occurred after 1 May, simple analysis of the banding period confirmed that the banding occurs twice per tidal cycle (resulting in an indicative freeze-over date of ∼8 May), and with this banding period, a correlation with the air temperature data has further refined this estimate to 11 May.

3. Comparison With A Sea-Ice Growth Model

We now demonstrate the utility of these data by comparing the measured

growth rates with the predictions from a simple growth-rate model. We use a simple heat flux model, with a steady state approximation where conductive heat flux is set equal to latent heat flux. We use air temperature data and an assumption of seawater freezing point temperature as a proxy for the temperature gradient at the base of the ice. Since a sudden change in air temperature can take up to several days to become close to steady state, we include a time delay factor, calculated in Appendix A. This allows for the time required for changes in air temperature to affect thermal gradients in the ice at the ice-water interface. The model uses air temperature data and a fitted freeze-in date to compute ice thickness and growth rate versus time, allowing us to plot growth rate versus thickness.

Full details of the model are: Scott Base EWS hourly air temperature data, T_a, from 03:00 on 14 May to 12:00 on 21 June 1999 were used as a proxy for the temperature at the upper surface of the sea ice. Seawater temperature, T_w, was assumed to be constant at -1.9°C. The thermal conductivity of sea ice was assumed constant at $k_{si} = 2.15$ W m^{-1} K^{-1} [*Pringle et al.*, 2006, 2007] using measured values for an average sea-ice temperature of $T_{si} = -13$°C, and an average sea ice salinity of 6 psu. The density of sea ice was taken to be constant at $\rho_{si} = 920$ kg m^{-3} [*Pringle et al.*, 2007]. Thermal diffusivity was taken to be constant at $\alpha_{si} = 8.89 \times 10^{-7}$ m^2 s^{-1}, where

$$\alpha_{si} = \frac{k_{si}}{\rho_{si} c_{si}} \tag{2}$$

Heat capacity was taken to be $c_{si} = 2.63$ kJ kg^{-1} K^{-1}, based on *Ono* [1967] with mean sea-ice salinity and temperature as above. Initial sea-ice thickness was set at 150 mm. At each time t, the time delay in seconds for thermal changes to diffuse through ice of thickness $H(t)$ was computed as (see Appendix A)

$$delay(t) = \frac{H(t)^2}{\pi \alpha_{si}} \tag{3}$$

The growth rates are given by equating the heat flux due to a steady state temperature gradient above the ice/water interface to the heat flux required to freeze seawater (equation 1, neglecting ocean heat fluxes). The time required for a sudden change in air temperature to affect the temperature gradient at the interface is included, giving the growth rate at time t as

$$\frac{dH}{dt} = \frac{k_{si}}{\rho_{si} L} \left(\left(\frac{T_w - T_a(t - delay(t))}{H(t)} \right) \right) \tag{4}$$

where $T_a(t - delay(t))$ is the air temperature at an earlier time $t - delay(t)$ and the latent heat of sea ice is taken to be constant at $L = 352$ kJ kg^{-1}, based on *Ono* [1967] with sea-ice salinity of $S = 6$ psu, mean sea-ice temperature as above and remaining variables as described for equation (1).

At each time t seconds, the sea-ice thickness was then updated as

$$H(t + \Delta t) = H(t) + \Delta t \frac{dH}{dt}$$

and Δt was set to 3600 s to obtain a time step size of 1 h.

By tuning the model in equation (4) to best fit the final depth measurement and the banding-derived growth rates, an assumed freeze-in date of the early hours of 14 May reproduces the sudden drop in growth rate at 600 mm depth. It also reproduces fluctuations in growth rates around 750 and 900 mm depth. However, at depths near 300–400 mm, the model predicts higher growth rates than the banding indicates. Using this model, final sea-ice thickness is calculated to be 1050 mm, which is a reasonable match to the measured final sea-ice thickness of 1100 ± 50 mm. The model output and banding-derived growth rates are illustrated in Figure 7.

4. Discussion

This study has clearly illustrated the analysis of visible banding to determine the growth rate of sea ice, opening the door for such a technique to yield growth-rate data at any landfast site where periodic tidal-driven banding is observed. The technique has several important advantages over real-time thickness measurements: it avoids the need for unsafe movement on the early ice cover and, even more importantly, the

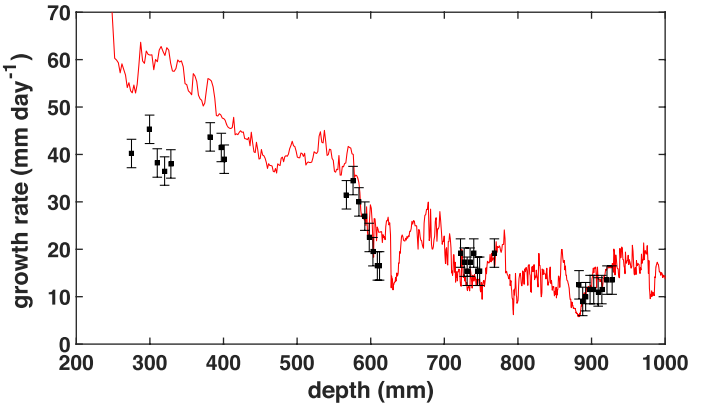

Figure 7. Growth rates versus total ice thickness, estimated from a delayed steady state model (solid line), compared with growth rates estimated from images of banding in sea-ice cores (symbols). The timing of sea-ice freeze-in at 150 mm thickness was tuned to early on 14 May 1999 to best match data and model.

data can be derived from ice cores collected during one late-season field trip. As well as being important for climate research, this method could contribute to the understanding of biological ecosystems within the ice [*Meiners et al.*, 2003], by providing a method to date depths in an ice core where particular organisms are observed or samples taken.

Visible periodic banding is not an unusual phenomenon in ice cores taken from coastal sea ice cover, where a similar analysis is likely to provide more detailed ground-truth growth-rate data for comparison with models. For that purpose, it is important to establish its utility even in situations where the tidal patterns are less well established. The present proof-of-concept study made use of a tidal pattern at a site where at least the tide height data, which contain information about the tidal period, are relatively complete, though that is not necessary to apply the analysis. Daily tidal periods, driven by the apparent motion of the sun and moon, are closely pinned to the range of 24.4 h $\pm$ 2%, and the single-cycle speed period is then within 2% of 6.1, 12.2, or 24.4 h, depending on whether the flow/ebb asymmetry is significant and whether the tides at the site are diurnal. Once the tidal pattern is known, it is a relatively simple matter to apply the analysis of Figure 5 above to relate the appropriate tidal period to even a relatively crude estimate of the typical surface temperature. A more sophisticated analysis will be necessary at sites where the tidal pattern is a combination of multiple tidal constituents with various periods, as both the banding period and the strength of the banding will vary throughout the cycle.

In addition to demonstrating the technique, we have performed a simple growth-rate calculation that compares well with the data, including with a rapid growth rate drop associated with warmer temperatures. The agreement is less than perfect, at shallow depths where the model ignores both the accumulation of snow that provides insulation from cooling by the atmosphere, and accumulation of salt, which would slow down rates of ice growth. The former reduces heat transport to the ice surface and the latter leads to salt accumulation and a reduced temperature at the ice-water interface, especially at early times when growth is relatively rapid [*McGuinness*, 2009]. With these limitations, the agreement is notable, lending confidence that the quasi-periodic banding in sea ice does indeed reflect the growth rate.

5. Conclusions

We have studied the quasi-periodic banding seen in a core of sea ice taken on the eastern side of McMurdo Sound, Antarctica in late 1999. The bands are most likely driven by variable under ice currents, leading to a banding pattern that relates directly to tidal flow, and allowing a determination of the rate of ice growth as a function of its thickness. The interpretation of the data has been supported by a directly measured thickness on 21 June, the absence of banding on neap-tide dates, and a sudden growth reduction that occurred after a fortuitous atmospheric warming. A simplified thermodynamic model of the growth rate shows reasonable agreement with the data, however the reliability of the model is compromised in the very early season when snow and salt accumulation, both of which are absent in the model, have a large impact on growth rates. Measurement of the periods in visible banding structure in first-year sea ice is a promising new tool, which can be exploited to follow columnar ice growth.

Appendix A: Delay Time Calculations

We calculate the time delay for a change in air temperature to affect the temperature gradient at the ice/water interface. This time delay is used to improve our growth model, which uses a steady state

approximation for this temperature gradient. So we derive a formula for the time taken after a sudden change in air temperature to reestablish a steady temperature profile in the sea ice.

We use the linear heat equation for the temperature of sea ice [e.g., *McGuinness*, 2009, *Carslaw and Jaeger*, 1959]

$$\frac{\partial T(z,t)}{\partial t} = \alpha_{si} \frac{\partial^2 T(z,t)}{\partial z^2}$$

with constant ice diffusivity α_{si} and ice thickness fixed at $z=H$.

Boundary conditions are: at the upper ($z=0$) and lower ($z=H$) surfaces of the sea ice, for $t > 0$, $T(0,t) = T_f$ and $T(H,t) = T_w$.

Initial conditions throughout the sea ice are

$$T(z,0) = T_i + (T_w - T_i)\frac{z}{H}$$

That is, the initial temperature at the ice surface is T_i and this changes suddenly at time zero to the new value T_f. Rescaling to a nondimensional temperature θ, using

$$\theta = \frac{(T - T_f)}{(T_f - T_i)} + \frac{(T_f - T_w)}{(T_f - T_i)}\frac{z}{H}$$

gives the same heat diffusion equation for θ, with zero boundary conditions at $z = 0, H$ for $t > 0$, and with initial conditions

$$\theta = -1 + \frac{z}{H}$$

Separation of variables gives the usual Fourier series solution

$$\theta = \frac{-2}{\pi}\sum_{m=1}^{\infty}\frac{1}{m}\sin\left(\frac{m\pi z}{H}\right)\exp\left(\frac{-m^2\pi^2\alpha_{si}t}{H^2}\right)$$

with the slope at $z = H$ being

$$\frac{d\theta}{dz} = \frac{-2}{L}\sum_{m=1}^{\infty}(-1)^m \exp\left(\frac{-m^2\pi^2\alpha_{si}t}{H^2}\right)$$

The slowest term to converge is when $m = 1$, giving the timescale

$$t_0 = \frac{H^2}{\pi^2\ \alpha_{si}}$$

for decay onto the new steady state, and numerical comparisons show that when the time reaches about πt_0 the transient solution and its slope has reached the new steady state to within about ten percent. That is, the delay time in seconds is approximately

$$delay = \frac{H^2}{\pi\ \alpha_{si}}$$

This gives a delay of 36 h for a depth of 600 mm.

Acknowledgments

The sea-ice cores used in this research were obtained under Event K131 supported by the then New Zealand Foundation for Research, Science and Technology under the Public Good Science Fund, with logistical support from Antarctica New Zealand. The authors are very grateful for Tim Haskell's 1999 sea ice science- and fieldwork-coordination, support, and guidance. I.J.S. was supported for the 1999 fieldwork through an Antarctica New Zealand Sir Robin Irvine Post-Graduate Scholarship and a Blair Trust scholarship, and she acknowledges subsequent financial support from University of Otago Research grants 106920 and 111030 and the support of Pat Langhorne that enabled her participation in this paper. J.-L.T. was supported through the Belgian Science Foundation (FNRS) and through the Belgian Antarctic Program (BELSPO, Science Policy Office). Jono Everts is thanked for his assistance in thermodynamic data analysis. The image file for the core photograph used in the analysis, and the resultant banding depths and growth rates can be found in the supporting information. The full set of core images can also be found at http://dev.ulb.ac.be/glaciol/MCMimages.zip.

References

Carslaw, H. S., and J. C. Jaeger (1959), *Conduction of Heat in Solids*, Oxford Univ. Press, Oxford.

Cole, D. M., H. Eicken, K. Frey, and L. H. Shapiro (2004), Observations of banding in first-year Arctic sea ice, *J. Geophys. Res.*, *109*, C08012, doi:10.1029/2003JC001993.

Doodson, A. (1924), Tidal observations: Reduction of the tide gauge records, in *Cape Evans, British Antarctic (Terra Nova) Expedition 1910–1913, Miscellaneous Data*, pp. 68–73, Harrison and Sons, London, U. K.

Eicken, H., C. Bock, R. Wittig, H. Miller, and H.-O. Poertner (2000), Magnetic resonance imaging of sea-ice pore fluids: Methods and thermal evolution of pore microstructure, *Cold Reg. Sci. Technol.*, *31*, 207–225.

Falconer, T. R., and A. R. Pyne (2004), Ice breakout history in Southern McMurdo Sound, Antarctica (1988–2002), *Antarct. Data Ser. 27*, Antarctic Research Centre in association with the School of Geography, Environment and Earth Sciences, Victoria, University of Wellington, New Zealand. [Available at http://www.victoria.ac.nz/antarctic/pdf/ADS27.pdf, downloaded on 8 Dec. 2010.]

Haines, E. M., R. G. Buckley and H. J. Trodahl (1997), Determination of the depth dependent scattering coefficient in sea ice, *J. Geophys. Res.*, *102*(C1), 1141–1151, doi:10.1029/96JC02861.
Heath, R. A. (1971a), Tidal constants for McMurdo Sound, Antarctica, *N. Z. J. Mar. Freshwater Res.*, *5*(2), 376–380.
Heath, R. A. (1971b), Circulation and hydrology under the seasonal ice in McMurdo Sound, Antarctica, *N. Z. J. Mar. Freshwater Res.*, *5*(3–4), 497–515.
Leonard, G. H., C. R. Purdie, P. J. Langhorne, T. G. Haskell, M. J. M. Williams, and R. D. Frew (2006), Observations of platelet ice growth and oceanographic conditions during the winter of 2003 in McMurdo Sound, Antarctica, *J. Geophys. Res.*, *111*, C04012, doi:10.1029/2005JC002952.
Light, B., G. A. Maykut, and T. C. Grenfell (2003), Effects of temperature on the microstructure of first-year sea ice, *J. Geophys. Res.*, *108*(C2), 3051, doi:10.1029/2001JC000887.
Mahoney, A. R., A. J. Gough, P. J. Langhorne, N. J. Robinson, C. L. Stevens, M. M. J. Williams, and T. G. Haskell (2011), The seasonal appearance of ice shelf water in coastal Antarctica and its effect on sea ice growth, *J. Geophys. Res.*, *116*, C11032, doi:10.1029/2011JC007060.
Mäkynen, M., and M. Similä (2015), Thin ice detection in the Barents and Kara seas with AMSR-E and SSMIS radiometer data, *IEEE Trans. Geosci. Remote Sens.*, *53*(9), 5036–5053.
McGuinness, M. J. (2009), Modelling sea ice growth, *ANZIAM J.*, *50*, 306–319, doi:10.1017/S1446181109000029.
Meiners, K., R. Gradinger, J. Fehling, G. Civitarese, and M. Spindler (2003), Vertical distribution of exopolymer particles in sea ice of the Fram Strait (Arctic) during autumn, *Mar. Ecol. Prog. Ser.*, *248*, 1–13.
National Institute of Water and Atmospheric Research (n.d.), *National Climate Database (CliDB)*. [Available at http://cliflo.niwa.co.nz/, Scott Base EWS Agent Number = 12740, accessed 30 Oct. 2014.]
Ono, N. (1967), Specific heat and fusion of sea ice, in *Physics of Snow and Ice: International Conference on Low Temperature Science 1966*, vol. *1*(1), edited by H. Oura, pp. 599–610, Inst. of Low Temp. Sci., Hokkaido Univ., Sapporo, Japan.
Pringle, D. J., H. J. Trodahl, and T. G. Haskell (2006), Direct measurement of sea ice thermal conductivity; no surface reduction, *J. Geophys. Res.*, *111*, C05020, doi:10.1029/2005JC002990.
Pringle, D. J., H. Eicken, H. J. Trodahl, and L. G. E. Backstrom (2007), Thermal conductivity of landfast Antarctic and Antarctic sea ice, *J. Geophys. Res.*, *112*, C04017, doi:10.1029/2006JC003641.
Smith, I. J., P. J. Langhorne, H. J. Trodahl, T. G. Haskell, and D. M. Cole (1999), Platelet ice: The McMurdo Sound Debate, in *Ice in Surface Waters—Proceedings of the 14th IAHR Symposium on Ice*, edited by H. T. Shen, pp. 371–378, A. A. Balkema, Rotterdam, Netherlands.
Smith, I. J., P. J. Langhorne, H. J. Trodahl, T. G. Haskell, R. Frew, and R. Vennell (2001), Platelet ice and the land-fast sea ice of McMurdo Sound, Antarctica, *Ann. Glaciol.*, *33*, 21–27, doi:10.3189/172756401781818365.
Smith, I. J., P. J. Langhorne, R. D. Frew, R. Vennell, and T. G. Haskell (2012), Sea ice growth rates near ice shelves, *Cold Reg. Sci. Technol.*, *83–84*, 57–70, doi:10.1016/j.coldregions.2012.06.005.
Trodahl, H. J., M. McGuinness, K. Collins, A. E. Pantoja, P. J. Langhorne, I. J. Smith, and T. G. Haskell (2000), Heat transport in McMurdo Sound first-year fast ice, *J. Geophys. Res.*, *105*(C5), 11,347–11,358.
Trodahl, H. J., S. O. F. Wilkinson, M. J. McGuinness, and T. G. Haskell (2001), Thermal conductivity of sea ice: Dependence on temperature and depth, *Geophys. Res. Lett.*, *28*(7), 1279–1282, doi:10.1029/1999JC000003.
Verbeke, V., J.-L. Tison, H. J. Trodahl, and T. G. Haskell (2002), Banding in McMurdo fast ice, in *Ice in the Environment: Proceedings of the 16th International Symposium on Ice, 2-6 December 2002*, Vol. *2*, edited by V. Squire and P. Langhorne, pp. 225–234, Univ. of Otago, Dunedin, New Zealand. [Available at http://dev.ulb.ac.be/glaciol/papers.html.]
Yu, Y., and D. A. Rothrock (1996), Thin ice thickness from satellite thermal imagery, *J. Geophys. Res.*, *101*(C10), 25,753–25,766, doi:10.1029/96JC02242.